

implemented, as well as electrode movement drive (EMD) and electrode movement mechanism (EMM). An electrical circuit in each phase is made up of an arc current sensor CS, an arc current set-point device (CSPD), an arc current regulator (CR) and a magneto-thyristor voltage regulator (MTVR).

MTVR consists of a pulse-phase control system PPCS and reactors R connected in parallel and two thyristors T connected in series in the power supply circuit of the furnace transformer FT.

The developed model takes into consideration all the major non-linearities of the power supply circuit of the three-phase arcs and rigidity parameters of the EMM kinematic scheme elements, adequately simulates parametric and coordinate perturbations in the power supply circuit and dependencies of the dynamic current/voltage diagrams of the arcs, as well as implements a user-friendly interface for changing the ACS structure, laws and parameters, carrying out mathematical experiments and statistical on-line processing of the results.

For the proposed double-loop ACS, it is important to study the dynamics indices of the EM coordinates' regulation and energy efficiency and electromagnetic compatibility indices of the electric arc furnace. In [3], a single-phase Simulink model of the arc power supply system was developed; hence, it has a low accuracy of simulating the arc currents' shape. The authors of [4] have presented a three-phase Simulink model of the arc furnace in the averaged coordinates, which does not allow simulate the changes of the arc voltage and current in the power circuit at the level of instantaneous values.

For this we developed a three-phase Simulink model of the double-loop ACS for the EM of the DSP-200 arc furnace in instantaneous coordinates, the structural block diagram of which is presented in Fig. 2.

The structural elements of the Simulink model simulating the elements of the three-phase arc power supply circuit, the three-phase arcs, the system of automatic regulation of the arc length and generation of random and determined

perturbations, and the computing blocks performing on-line statistical processing of the obtained EM coordinates' changes for the melting process are described in [5].

The power elements of the magneto-thyristor voltage regulator are presented in the Simulink model (Fig. 2) by the block MTVR (green), its phase channels of the pulse-phase control system PPCS shows the developed structural Simulink model of one phase of MTVR with three parallel thyristor-reactor groups (PTRG), and Fig. 4 presents the detailed Simulink model of one PTRG.

The PTRG Simulink model shown in Fig. 3 consists of three reactors R connected in series, each of which is connected with a pair of anti-parallel thyristors T. The furnace load currents (i.e., arc currents) are regulated by changing the thyristor control angles, which influences the equivalent inductance of each reactor. The thyristor control angles are formed by PPCS in the function of the output signals of the arc current regulators CR (Fig. 1, Fig. 2).

The integral criterion of the quality of EM coordinates regulation is the arc current dispersion. When dealing with random perturbations, the arc current dispersion is determined mainly by the EM coordinates' ACS operation speed, level of independence of the phase channels of regulation, control law for EM and dependency of the external static characteristic of the arc furnace $I_a(U_a)$. The natural external static characteristic of the arc furnace $I_a(U_a)$ is presented in Fig. 5, curve 1. The high-speed circuit enables various artificial external characteristics $I_a(U_a)$ of the arc furnace to be formed and the corresponding EM optimal control strategies to be implemented.

One of the strategies using a double-loop control system for EM is the stabilization of the current at the level of a set-point value. Such optimal control strategy is implemented by forming an artificial external characteristic $I_a(U_a)$ of the arc furnace by a high-speed electrical circuit with a segment of arc current stabilization $I_a=const$ (Fig. 5, curve 2).

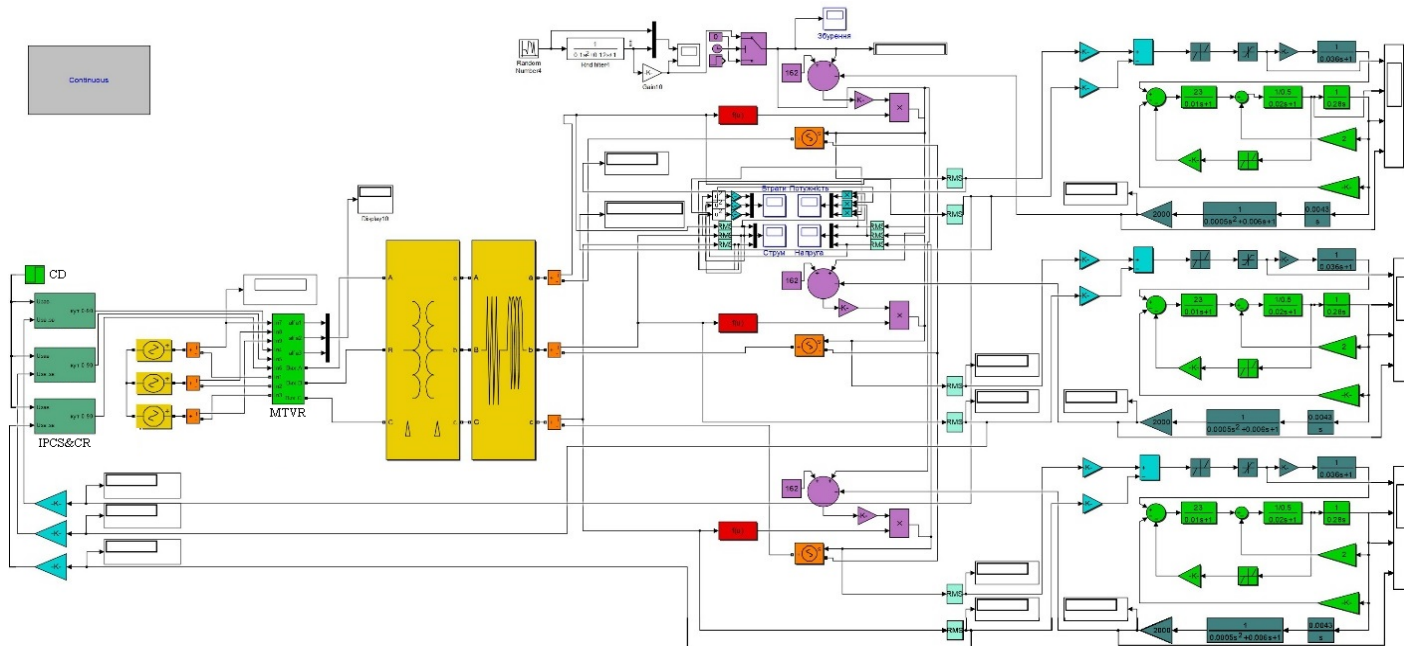


Fig. 2. Block diagram of the three-phase instantaneous coordinates Simulink model of ACS for EM of the DSP-200 furnace

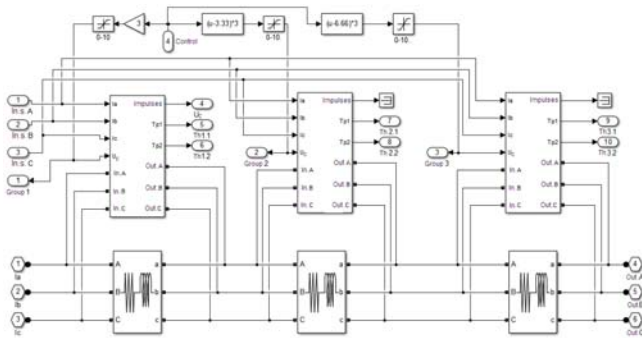


Fig. 3. Simulink-model of magneto-thyristor voltage regulator with three parallel thyristor-reactor groups

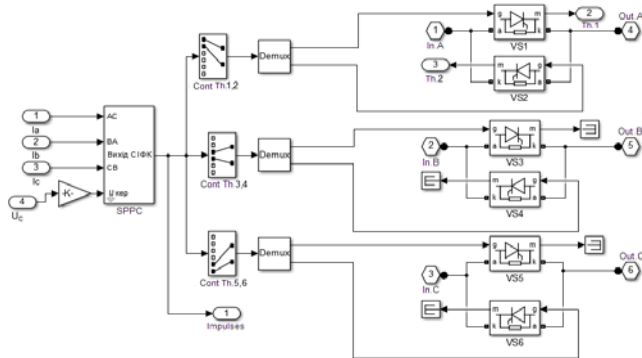


Fig. 4. Simulink model of one parallel TRG with the pulse-phase control system and power thyristors

The use of this strategy leads to in the minimization of arc current dispersion $D_{I_a} \rightarrow \min$, reduced power loss in the power supply circuit of the furnace, decreased reactive power and its dispersion.

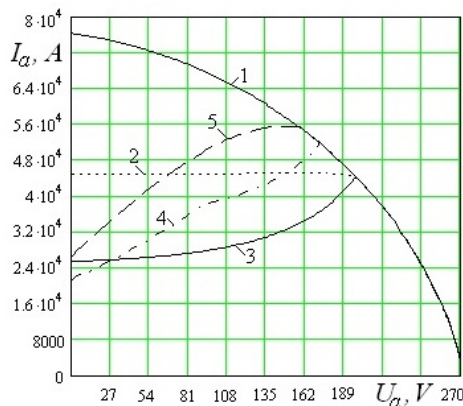


Fig. 5. External characteristics $I_a(U_a)$ of EAF

The regulation law for the inductance of the reactor MTVR for the strategy $D_{I_a} \rightarrow \min$ is presented as

$$(1) \quad x_p^{I_a}(U_a) = \frac{\sqrt{U_{2f}^2 - U_a^2 - 2rU_a I_{a,st} - r^2 I_{a,st}^2}}{I_{a,st}} - x$$

For the proposed double-loop ACS structure (Fig. 1), other laws of arc current control were devised. As an example, Fig. 5 shows artificial external characteristics 3, 4, 5 of the furnace DSP-200, which correspond to different strategies of EM optimal control: curve 3 presents optimization by the criterion of the reactive power dispersion minimum $Q \rightarrow \min$, curves 4 and 5 correspond to the multi criteria EM control strategy, whose partial criteria are the arc power maximization (i.e., the furnace output) $P_a \rightarrow \max$, minimization of the electrical loss power in the power supply circuit of the three-

phase arcs (i.e., in the low-voltage circuit of the furnace) $P_{el} \rightarrow \min$, reactive power dispersion minimization and minimization of the specific losses of electrical power $W \rightarrow \min$. These partial criteria in the generalized functional of the multi criteria optimization are normalized by the respective weight factors.

The developed Simulink model was used to study the dynamics of EM coordinates' regulation in the structure of the double-loop ACS for the cases of symmetrical and non-symmetrical perturbations of the arc length in the arc spaces, continuous random perturbations with different parameters of stochastic characteristics, as well as to estimate the performance indices when using different laws of control – differential, impedance, as well as one based on the current and voltage deviation laws.

Fig. 6 shows time dependencies of the arc current during implementation of regulation for symmetrical three-phase short circuit using the one-loop EM ACS for control based on the arc current deviation law a) for regulation the arc current by the high-speed electrical circuit with the proportionally integral regulator CR of the arc current b) and for the case of the functioning of the double-loop EM ACS with the above-mentioned law based on the arc current deviation and PI structure of the arc current regulator CR of the high-speed circuit (Fig. 1). Due to using the high-speed circuit in the ACS, the duration of the arc current regulation is reduced 30-40 times. The insignificant extension of the regulation time in the experiment in Fig. 6,c as compared to Fig. 6,b can be explained by the single-phase symmetry of the elements of the low-voltage circuit of EAF, which is displayed for the control under the arc-deviation law.

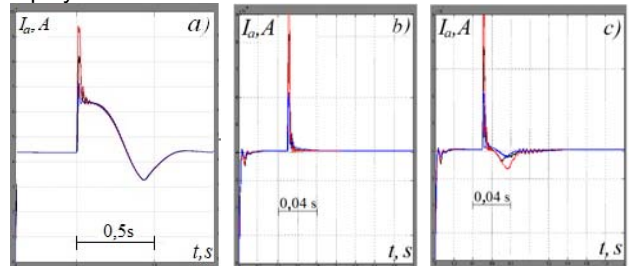


Fig. 6. Time dependencies of the current $I_a(t)$ for regulating the symmetrical short circuit a) by the single-loop ACS with the high-speed circuit b) and by the double-loop ACS for EM control based on the current deviation

Fig. 7 presents similar time dependencies, but for the regulation of non-symmetrical perturbation – short circuit in phase A.

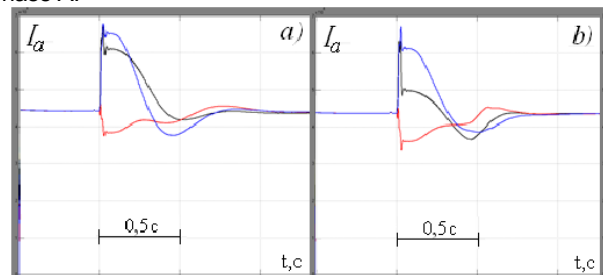


Fig.7. Time dependencies of arc currents for regulating the non-symmetrical short circuit in phase A by the double-loop ACS for different laws of arc length regulation and PI regulator of arc currents of the high-speed circuit

Fig. 8 presents quasi steady-state processes of change of the arc currents $I_a(t)$ for the regulation of random perturbations $f(t)$ by the double-loop EM ACS (the electromechanical arc power regulator ARDM-T-12 of the furnace DSP-200 and high-speed circuit of arc current regulation (Fig. 1)) at the beginning of the technological stage of solid fusion mixture melting,

whereas Fig. 9 shows these same processes $I_a(t)$ at the end of this stage.

The analysis of the dependencies $I_a(t)$ presented in Fig. 8 and Fig. 9 shows quality limitation of the arc current by the value $I_{a,st}=43.97\text{kA}$. Due to this, the arc current dispersion is reduced 4-6-times as compared to the operation of the single-loop structure (the power regulator ARDM-T-12).

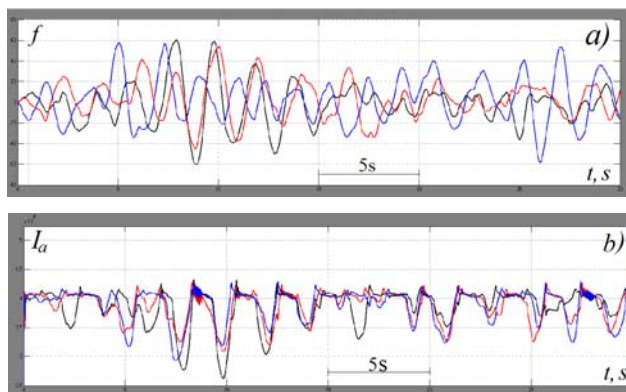


Fig. 8. Perturbations of the arc length $f(t)$ in the phases a) and the respective arc currents $I_a(t)$ b) of the double-loop ACS at the beginning of the solid fusion mixture melting stage

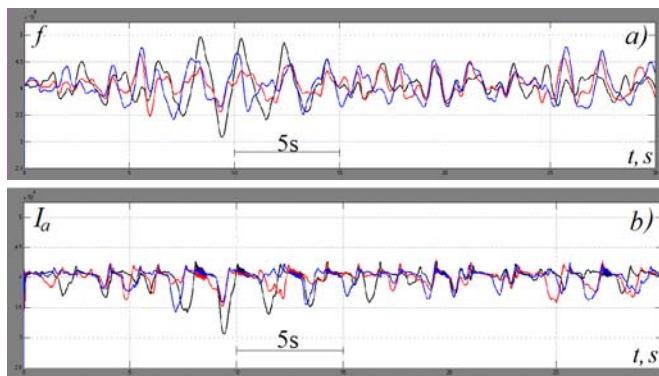


Fig. 9. Perturbations of the arc length $f(t)$ in the phases a) arc currents $I_a(t)$ b) when using the double-loop ACS at the end of the solid fusion mixture melting stage

Reducing dispersion and increasing the speed of arc current control stabilizes the process of reactive power consumption and reduces its average value. At the same time, the power factor increases, power losses in the power supply system and the power circuit of the arc furnace are reduced, as well as deviations, voltage drops and flicker dose are reduced at the point of connection of the EAF to the electrical network.

The developed Simulink model was also used to study the harmonic composition of the arc currents for the operation of different structures of EM ACS, laws of formation of the control signal for electrodes movement and effects of arc length perturbations with various parameters of stochastic perturbations. Fig. 10 presents the diagram of the averaged amplitudes of the characteristic harmonics of the arc currents for the interval of the stochastic arc length perturbation's regulation $T=60\text{s}$ by the double-loop EM ACS and formation of the control signal according to the differential law for one TRG (Fig. 10,a) and three parallel TRG (Fig. 10,b) (the first harmonic – 100%, shown in a different scale).

As the harmonics analysis reveals, when using three parallel thyristor-rector groups, the fifth and seventh harmonics are reduced 4-fold, whereas the other harmonics of the arc currents are reduced 1.5-3-fold.

Conclusions

1. A structural three-phase Simulink model in the instantaneous coordinates of the double-loop control system for EM of the electric arc furnace was developed. The model offers a wide range of useful functionalities for computer-aided studies of various structures and for different parameters of EM ACS, different control laws and perturbations' characteristics. It also enables the performance of the online statistical processing of EM coordinates' variation, energy efficiency and electromagnetic compatibility indices, especially the harmonic analysis of the arc current and voltage and power supply network.

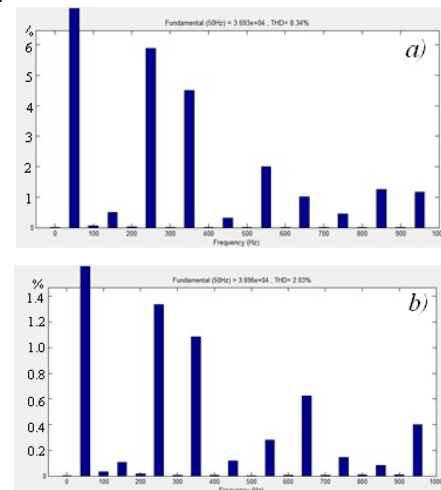


Fig.10. Amplitudes of the arc current harmonics for using one PTRG a) and three PTRG b) in MTRV for the differential control law

2. The results of the study showed a significant comprehensive improvement of the indices of arc current regulation dynamics and the indices of electromagnetic compatibility of the EAF modes and power supply network. It was shown that the functioning of the high-speed circuit of the arc current regulation helped achieve a significant reduction of the arc current dispersion and the level of the higher-order harmonics of the arc currents.

Authors: prof. dr hab. inż. Orest Lozynskiy, Institute of Power Engineering and Control Systems, Lviv Polytechnic National University, Ukraine, Lviv, ul.S.Bandery, 12. E-mail: orest.y.lozynskiy@lpnu.ua; prof. dr hab. inż. Yaroslav Paranchuk, Institute of Power Engineering and Control Systems, Lviv Polytechnic National University, Ukraine, Lviv, ul.S.Bandery, 12. E-mail: y.paranchuk@yahoo.com; prof. dr hab. inż. Petro Stakhiv, Institute of Information Technology, Lodz University of Technology, Poland, Lodz, Stefan Żeromskiego 116, 90-924 Łódź E-mail: petro.stakhiv@p.lodz.pl

REFERENCES

- 1 Bedin M., Romano M.. Arc furnace with supply through saturated reactor // *Electrometallurgy*. – 2004. - №4. - pp.15-20.
- 2 O.Yu.Lozynskii, Ya.S.Paranchuk. System for the Optimum Control of the Electrical Conditions of an Arc Furnace Powered through a Controlled Reactor // *Russian Metallurgy (Metally) English Translation of Elektrometallurgiya* — №8. – 2007. – Pp.737-743.
- 3 A.N.Chernenko, V.V.Vakhnina, S.H.Martynova. Dynamic model of furnace arc in Matlab (Simulink) // *Science vector of TGU*. 2015. № 2 (32-1). Pp.58-68.
- 4 Benoit Boulet, Gino Lalli and Mark Ajersch. Modeling and Control of an Electric Arc Furnace // *Proceedings of the American Control Conference Denver, Colorado June 4-6, 2003*. Pp.3060-3064.
- 5 Lozynskiy O., Paranchuk Y., Kobylanskyi O. Computer Modeling of Electric Arc Furnace Electrode Position Control System. *Proceedings of the XII-th International CSIT-2017*. - Lviv, 2017. – Pp.142-145.